J. Am. Chem. Soc. 1994, 116, 295–301

Role of the Template Layer in Organizing Self-Assembled Films: Zirconium Phosphonate Monolayers and Multilayers at a Langmuir–Blodgett Template

Houston Byrd,[†] Scott Whipps,[†] John K. Pike,[†] Jingfei Ma,[‡] Stephen E. Nagler,[‡] and Daniel R. Talham[*,†]

Contribution from the Departments of Chemistry and Physics, University of Florida, Gainesville, Florida 32611-2046

Received August 16, 1993[●]

Abstract: Organophosphonate monolayer and multilayer films have been prepared by self-assembly of organophosphonic acid molecules at a zirconium octadecylphosphonate Langmuir–Blodgett (LB) film. Infrared and XPS analyses of the zirconated LB template layer demonstrate that it is well-ordered and close-packed with a Zr:P ratio of 1:1, indicating that a surface with a high density of zirconium binding sites is produced. Polarized ATR-FTIR measurements reveal that the alkyl chains in the LB template layer are tilted by 31° from the surface normal. Octadecylphosphonic acid is self-assembled at the zirconated LB template to produce a zirconium octadecylphosphonate bilayer. ATR-FTIR spectroscopy of the C–H stretching bands indicates that the self-assembled layer is close-packed and that the alkyl chains are in an all-trans conformation. XPS analysis shows that the bilayer possesses a Zr:P ratio of 1:2 and that every template Zr^{4+} site binds one octadecylphosphonic acid molecule from solution. Contact angle measurements on the completed bilayer reveal an advancing contact angle of 110 ± 1°. The tilt angle of the alkyl chains in the self-assembled layer is 22°, as determined by polarized ATR-FTIR, which is contrasted to the 5° tilt angle seen if the octadecylphosphonic acid capping layer is deposited as an LB film. Multilayer films of 1,10-decanediyldiphosphonic acid (DDPA) are also assembled at the zirconated LB template. The layer-by-layer deposition is monitored by integrating the intensity of the $\nu_a(CH_2)$ band after each deposition cycle. In the first few layers, the diphosphonic acid molecules bridge zirconium sites on the template layer, but a constant rate of deposition is achieved after three or four layers. Analysis of the fwhm of the $\nu_a(CH_2)$ band indicates that close-packed films are not produced. The rigid α,ω-diphosphonic acid quaterthiophenediphosphonic acid (QDP) is also assembled layer-by-layer at the zirconated LB template. UV–vis analysis indicates that the same amount of material is deposited after each deposition cycle. X-ray diffraction from 10 layers of QDP reveals a d spacing of 20.19 Å, demonstrating the layered nature of the film. The QDP molecules are oriented nearly perpendicular to the surface.

Introduction

The promise of directing the properties of systems by controlling the architecture, orientation, and density of molecules within organized assemblies is currently an important driving force in many aspects of chemical research. In developing organized thin films, the Langmuir–Blodgett[1–3] (LB) technique and various procedures for the "self-assembly" (SA) of organic molecules at surfaces[3–7] are examples of methods that produce functional assemblies through the purposeful manipulation of molecules. Applications that make use of thin films often require multilayers, and while depositing multilayer LB films is straightforward, there are only a few self-assembly routes to multilayer films.[8–17] The potential advantages of self-assembled multilayers include less complicated processing, and the structural stability afforded by covalent linkages between the layers. A remaining question,[18,19] however, is what degree of orientational and position order can be achieved among molecules in self-assembled multilayer structures.

The first report of multilayer films prepared by organic self-assembly was published by Sagiv and co-workers.[8] In this procedure, a monolayer of 15-hexadecenyltrichlorosilane (HTS) is adsorbed onto an oxide surface followed by activation of the terminal olefin to produce a surface of hydroxyl functionalities. The OH-terminated surface can adsorb another layer of HTS, and by repetition of the process multilayer films can be constructed. Several other groups[9,10] have followed similar procedures in order to prepare multilayer films. Tillman et al.[9] also used Si–O linkages to prepare multilayer films of methyl 23-(trichlorosilyl)tri-

---

[*] Address correspondence to this author.

[†] Department of Chemistry.

[‡] Department of Physics.

[●] Abstract published in *Advance ACS Abstracts*, December 1, 1993.

(1) Gaines, G. J. *Insoluble Monolayers at Liquid-Gas Interfaces*; Wiley-Interscience: New York, 1966.

(2) *Langmuir-Blodgett Films*; Roberts, G. G., Ed.; Plenum Press: New York, 1990.

(3) Ulman, A. *An Introduction to Ultrathin Organic Films: From Langmuir-Blodgett to Self-Assembly*; Academic Press: Boston, MA, 1991.

(4) Bigelow, W. C.; Pickett, D. L.; Zisman, W. A. *J. Colloid Sci.* **1946**, *1*, 513–538.

(5) Maoz, R.; Sagiv, J. *J. Colloid Interface Sci.* **1984**, *100*, 465–496.

(6) Bain, C. D.; Troughton, E. B.; Tao, Y.-T.; Evall, J.; Whitesides, G. M.; Nuzzo, R. G. *J. Am. Chem. Soc.* **1989**, *111*, 321–335.

(7) Wasserman, S. R.; Tao, Y.-T.; Whitesides, G. M. *Langmuir* **1989**, *5*, 1074–1087.

(8) Netzer, L.; Sagiv, J. *J. Am. Chem. Soc.* **1983**, *105*, 674–676.

(9) Tillman, N.; Ulman, A.; Penner, T. L. *Langmuir* **1989**, *5*, 101–111.

(10) Li, D.; Ratner, M. A.; Marks, T. J.; Zhang, C.-H.; Yang, J.; Wong, G. K. *J. Am. Chem. Soc.* **1990**, *112*, 7389–7390.

(11) Lee, H.; Kepley, L. J.; Hong, H.-G.; Mallouk, T. E. *J. Am. Chem. Soc.* **1988**, *110*, 618–620.

(12) Lee, H.; Kepley, L. J.; Hong, H.-G.; Akhter, S.; Mallouk, T. E. *J. Phys. Chem.* **1988**, *92*, 2597–2601.

(13) Akhter, S.; Lee, H.; Hong, H.-G.; Mallouk, T. E.; White, J. M. *J. Vac. Sci. Technol.* **1989**, *7*, 1608–1613.

(14) Hong, H.-G.; Sackett, D. D.; Mallouk, T. E. *Chem. Mater.* **1991**, *3*, 521–527.

(15) Kepley, L. J.; Sackett, D. D.; Bell, C. M.; Mallouk, T. E. *Thin Solid Films* **1992**, *208*, 132–136.

(16) Cao, G.; Hong, H.-G.; Mallouk, T. E. *Acc. Chem. Res.* **1992**, *25*, 420–427.

(17) Evans, S. D.; Ulman, A.; Goppert-Berarducci, K. E.; Gerenser, L. J. *J. Am. Chem. Soc.* **1991**, *113*, 5866–5868.

(18) Schilling, M. L.; Katz, H. E.; Stein, S. M.; Shane, S. F.; Wilson, W. L.; Buratto, S.; Ungashe, S. B.; Taylor, G. N.; Putvinski, T. M.; Chidsey, C. E. D. *Langmuir* **1993**, *9*, 2156–2160.

(19) Frey, B. L.; Hanken, D. G.; Corn, R. M. *Langmuir* **1993**, *9*, 1815–1820.

0002-7863/94/1516-0295$04.50/0 © 1994 American Chemical Society

cosanoate (MTST). By first preparing a monolayer of MTST and then converting the terminating esters to hydroxyl groups, they were able to deposit multilayer films layer-by-layer. Marks and co-workers[10] used similar methodologies to prepare chromophoric multilayer films.

Procedures have also been developed where self-assembled organic layers are linked by transition metal ions.[11-17] Mallouk and co-workers[11-16] demonstrated a method for one-layer-at-a-time depositions of α,ω-diphosphonic acids that takes advantage of the strong affinity of phosphonate (or phosphate) groups for the Zr^{4+} ion. In this procedure, a molecule bearing the phosphonic acid functionality is adsorbed to a surface and layers are built up by alternately adsorbing Zr^{4+} ions and α,ω-diphosphonic acid molecules from solution. Thin films formed in this way have been used as the dielectric in metal–insulator–semiconductor and metal–insulator–metal devices.[15] Katz and co-workers[18,20-23] have adapted this procedure to prepare films containing oriented assemblies of a wide variety of functionalized molecules. Among the properties demonstrated in such films are interlayer electron transfer[23] and second harmonic generation.[22]

Several methods have been described for preparing the initial phosphonate-derivatized surface.[11,12,21,22] The original work adsorbed 3-(hydroxydimethylsilyl)propylphosphonic acid to oxide surfaces[11,12] and the disulfide $[S(CH_2)_4PO_3H_2]_2$ to Au electrodes.[12] Another approach involves reacting $POCl_3$ with the polymer derived from 3-(aminopropyl)trimethoxysilane.[21,22] Efforts to increase the organization of the surface layer have taken advantage of the "self-assembling" quality of longer alkyl chain derivatives. (Triethoxysilyl)nonadecyl acetate[18] and (triethoxysilyl)octadecyl bromide[24] have been self-assembled to oxide surfaces and subsequently transformed to phosphonic acid derivatives on the surface. Katz et al.[18] have also directly deposited 19-thiononadecylphosphonic acid onto Au surfaces for the buildup of zirconium phosphonate multilayers.

In a previous report[25] describing the use of LB methods to prepare single-layer analogs of the solid-state zirconium phosphonates, we detailed a procedure for zirconating an LB monolayer of octadecylphosphonic acid. The LB layer provides an organized array of phosphonate sites at the surface that we have shown is close-packed and coordinates one zirconium ion per phosphonate group.[25] We have found that this LB method produces a more organized phosphonate derivatized surface than do any of the SA methods that we have investigated. In the present paper, we describe how this zirconated LB layer can be used as a "template" for self-assembling organophosphonates. Starting with a well-characterized and ordered "template" layer, we can quantify subsequent self-assembly steps and learn how the order and packing density of the template layer extends to the built-up layers. To this end, we have studied the self-assembly of a monolayer of octadecylphosphonic acid at the LB template, as well as the buildup of multilayer films using 1,10-decanediyldiphosphonic acid, in analogy to the original procedure described by Mallouk.[11,12] We have also investigated use of the LB template for depositing quaterthiophenediphosphonic acid (QDP) which

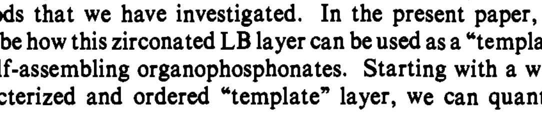

is a rigid molecule developed by Katz and co-workers[21] for the purpose of building up zirconium phosphonate multilayers. We monitor the deposition processes by FTIR, contact angle, XPS, UV–vis, and X-ray diffraction. We show that a high degree of orientational order can be achieved in self-assembled organophosphonate layers and that the organization of functional sites in the initial template layer is an important factor. For example, the rigid QDP molecule assembles with sufficient orientational order at the zirconated LB template such that Bragg diffraction is observed from 10 layers self-assembled onto a planar surface.

Experimental Section

Materials. Octadecylphosphonic acid ($C_{18}H_{39}O_3P$) and 1,10-decanediyldiphosphonic acid ($C_{10}H_{24}O_6P_2$, DDPA) were synthesized from octadecyl bromide and 1,10-dibromodecane, respectively, by the Michaelis–Arbuzov[26] reaction, followed by acid hydrolysis. Quaterthiophenediphosphonic acid (QDP) was provided by Dr. Howard Katz.[21] Zirconyl chloride, 98%, was used as purchased from Aldrich (Milwaukee, WI).

Substrates. Single crystal (100) silicon wafers, purchased from Semiconductor Processing Co. (Boston, MA), were used as deposition substrates. Silicon attenuated-total-reflectance (ATR) crystals (50 mm × 10 mm × 3 mm), purchased from Wilmad Glass (Buena, NJ), were used as substrates for all infrared experiments. Silicon ATR crystals were parallelograms, with a 45° angle of incidence with respect to the parallel faces. The silicon substrates were cleaned using the RCA cleaning procedure[27] then dried under N_2. Octadecyltrichlorosilane- (OTS-) coated surfaces were prepared by placing the cleaned substrates in a 2% solution of OTS in hexadecane for 30 min. After the substrates were rinsed with chloroform to remove any excess hexadecane, they were dried under flowing N_2. Glass microscope slides (76.4 mm × 25.4 mm × 1 mm), purchased from Fisher Scientific, were used in all UV–vis experiments. The glass substrates were cleaned and prepared by following the same procedure used for the silicon substrates.

Methods. The Langmuir–Blodgett experiments were performed using KSV Instruments (Stratford, CT) Teflon-coated LB troughs with hydrophobic barriers. A Barnstead NANOpure purification system produced water with a resistivity of 18 MΩ cm for all experiments. Depositions were carried out using the KSV 3000 system, and in all cases films were compressed linearly at a rate of 5 (mN/m)/min at room temperature. For the depositions, a target pressure of 20 mN/m was maintained with deposition speeds of 10 mm/min.

Infrared spectra were recorded with a Mattson Instruments (Madison, WI) Research Series-1 Fourier transform infrared (FTIR) spectrometer using a narrow-band mercury cadmium telluride detector. A Harrick (Ossining, NY) TMP stage was used for the ATR experiments. Polarized FTIR-ATR spectra were taken with s- and p-polarized light. All spectra consist of 1000 scans at 2.0-cm^{-1} resolution and were ratioed to the OTS-covered substrates or the appropriate s- or p-polarized background.

Advancing contact angle measurements were measured with a Ramé-Hart (Mountain Lakes, NJ) NRL contact angle goniometer, Model 100-00. A 250-μL syringe was used to dispense a fixed-volume water drop to the surface.

X-ray photoelectron spectra were obtained using a Perkin-Elmer PHI 5000 Series spectrometer. All spectra were taken using the Mg Kα line source at 1253.6 eV. The spectrometer has a typical resolution of 2.0 eV, with anode voltage and power settings of 15 kV and 300 W, respectively. Typical operating pressure was 5×10^{-9} atm. Survey scans were performed at a 45° takeoff angle with a pass energy of 89.45 eV. Multiplex scans, 140 scans at each peak, were run over a 20–40-eV range with a pass energy of 37.75 eV. In all cases, the observed relative intensities are determined from experimental peak areas normalized with atomic and instrument sensitivity factors.[28,29]

UV–vis spectra were obtained with a Hewlett-Packard 8452A diode array spectrometer. The incident beam was aligned perpendicular to the substrate.

Low-angle X-ray diffraction was performed with a Rigaku 18-kW rotating-anode diffractometer. The X-ray source was the Cu Kα line, λ = 1.54 Å, which was first passed through a graphite monochromator. The diffracted X-ray beam was passed through a graphite analyzer before detection.

---

(20) Putvinski, T. M.; Schilling, M. L.; Katz, H. E.; Chidsey, C. E. D.; Mujsce, A. M.; Emerson, A. B. *Langmuir* **1990**, *6*, 1567–1571.

(21) Katz, H. E.; Schilling, M. L.; Chidsey, C. E. D.; Putvinski, T. M.; Hutton, R. S. *Chem. Mater.* **1991**, *3*, 699–703.

(22) Katz, H. E.; Scheller, G.; Putvinski, T. M.; Schilling, M. L.; Wilson, W. L.; Chidsey, C. E. D. *Science* **1991**, *254*, 1485–1487.

(23) Ungashe, S. B.; Wilson, W. L.; Katz, H. E.; Scheller, G. R.; Putvinski, T. M. *J. Am. Chem. Soc.* **1992**, *114*, 8717–8719.

(24) Crews, M. L. Masters Thesis, University of Florida, 1992.

(25) Byrd, H.; Pike, J. K.; Talham, D. R. *Chem. Mater.* **1993**, *5*, 709–715.

(26) Bhattacharya, A. K.; Thyagarajan, G. *Chem. Rev.* **1981**, *81*, 415–430.

(27) Kern, W. *J. Electrochem. Soc.* **1990**, *137*, 1887–1892.

(28) Wagner, C. D.; Davis, L. E.; Zeller, M. V.; Taylor, J. A.; Raymond, R. M.; Gale, L. H. *Surf. Interface Anal.* **1981**, *3*, 211.

Scheme 1. Preparation of a Zirconated Langmuir–Blodgett Template Layer

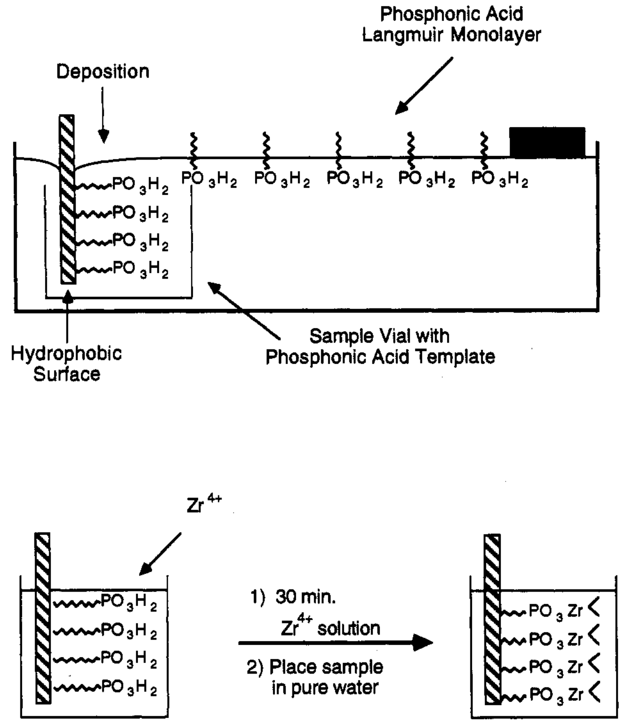

Results and Discussion

The Template Layer. The preparation and characterization of the zirconated LB template layer (Scheme 1) that is used in the SA experiments reported here have been described in detail in a previous paper.[25] Briefly, an octadecylphosphonic acid Langmuir monolayer is transferred tail-to-tail to an OTS-covered substrate by dipping the substrate down through the air/water interface and into a vial which is immersed in the trough. The vial containing the phosphonic acid-coated substrate is then removed from the trough, and $ZrOCl_2$ is added to the vial. The binding of zirconium ions to the LB template layer is complete within 30 min, and the substrate is rinsed with water before reaction with solutions of the organophosphonates. According to XPS,[25] the Zr:P ratio in the zirconated template film is 1:1, revealing that each phosphonic acid in the LB film binds a Zr^{4+} ion. ATR-FTIR of the zirconated template indicates that the octadecylphosphonate molecules in the template layer are close-packed. The infrared spectrum from 3100 to 2600 cm^{-1} for the template layer is shown in Figure 1 (top), and three bands are resolved:[5,30] the asymmetric methyl stretch ($\nu_a(CH_3)$) at 2960 cm^{-1}, the asymmetric methylene stretch ($\nu_a(CH_2)$) at 2918 cm^{-1}, and the symmetric methylene stretch ($\nu_s(CH_2)$) at 2852 cm^{-1}. The appearance of $\nu_a(CH_2)$ at 2918 cm^{-1} with a fwhm of 20 cm^{-1} is the same as is seen in solid octadecylphosphonic acid[25] and indicates that the alkyl chains possess an all-trans conformation and are close-packed. An increase in the number of gauche bonds will shift $\nu_a(CH_2)$ to higher energy,[5,30] while orientational disorder[5,31] will increase the fwhm.

Polarized ATR-FTIR[32,33] was used to determine the molecular axis tilt angles (from the normal) of the octadecylphosphonate molecules in the zirconated LB template layer. In this experiment, the absorbance of the $\nu_a(CH_2)$ band was recorded with s- and p-polarized light. From the absorbance data, a dichroic ratio, D, defined as

$$D = (A_x + A_z)/A_y$$

was calculated where $(A_x + A_z)$ is the absorbance with p-polarized light and A_y is the absorbance with s-polarized light. The molecular axis tilt angles are determined from the dichroic ratio[32,33] and are listed in Table 1 and illustrated in Scheme 2. The tilt angle for the zirconated LB template is 31°. This is precisely the tilt angle predicted from a SYBYL molecular modeling structure of zirconium octadecylphosphonate.[25] In the model, the crystallographic coordinates for α-$Zr(HPO_4)_2 \cdot H_2O$[34] are used to model the Zr–O_3P binding and alkyl chains are grafted on in place of the phosphate OH groups. The tilt angle results from the P–C bond orienting perpendicular to the zirconium ion plane. The large tilt angle observed for the LB template layer suggests that this layer relaxes in the pure water subphase after it is transferred. Addition of zirconium ions then cross-links the layer and holds it in place. Together, XPS and ATR-FTIR analyses reveal that the zirconated LB template layer consists of a high density of evenly-spaced Zr^{4+} sites on an organized octadecylphosphonic acid surface. The low solubility of zirconium

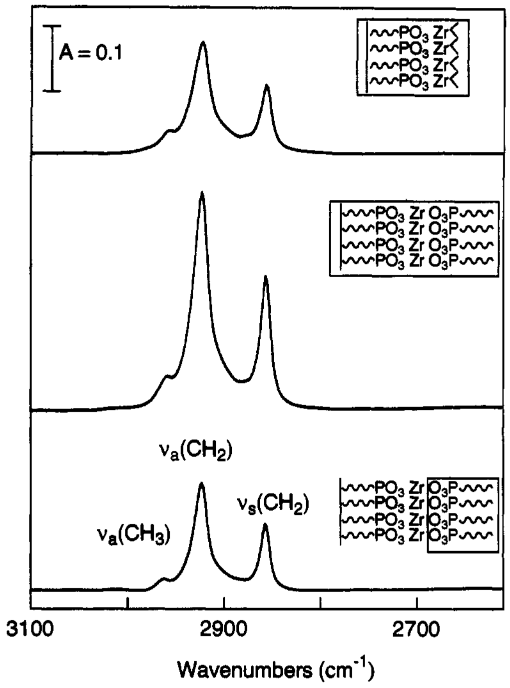

Figure 1. ATR-FTIR spectra monitoring the self-assembly of octadecylphosphonic acid at a zirconated template: the zirconated LB template layer (top), the self-assembled zirconium octadecylphosphonate bilayer (middle), the self-assembled octadecylphosphonic acid layer only (bottom). For each spectrum the $\nu_a(CH_2)$ band appears at 2918 cm^{-1} and possesses a fwhm of 20 cm^{-1}. The intensity of the self-assembled layer spectrum is identical to that of the template layer spectrum, and the intensity of the bilayer spectrum is double that of the template layer.

Table 1. Polarized FTIR-ATR Data for Zirconium Octadecylphosphonate Films

film type	dichroic ratio[a]	molecular axis tilt, deg[b]
zirconated LB template layer	1.08	31 ± 5
self-assembled octadecylphosphonic acid capping layer	1.0	22 ± 5
Langmuir–Blodgett octadecylphosphonic acid capping layer	0.92	5 ± 5

[a] Dichroic ratio is defined as $(A_x + A_z)/A_y$. [b] Tilt angle is defined as the tilt of the molecular axis with respect to the surface normal.

---

(29) *5000 Series ESCA Systems Version 2.0 Instruction Manual*; Perkin-Elmer Physical Electronics Division: Eden Prairie, MN, 1989.

(30) Porter, M. D.; Bright, T. B.; Allara, D. L.; Chidsey, C. E. D. *J. Am. Chem. Soc.* **1987**, *109*, 3559–3568.

(31) Wood, K. A.; Snyder, R. G.; Strauss, H. L. *J. Chem. Phys.* **1989**, *91*, 5255–5267.

(32) Haller, G. L.; Rice, R. W. *J. Phys. Chem.* **1970**, *74*, 4386–4393.

(33) Tillman, N.; Ulman, A.; Schildkraut, J. S.; Penner, T. L. *J. Am. Chem. Soc.* **1988**, *110*, 6136–6144.

(34) Clearfield, A.; Smith, G. D. *Inorg. Chem.* **1969**, *8*, 431–436.

Scheme 2. Molecular Axis Tilt Angles in Zirconium Octadecylphosphonate Films

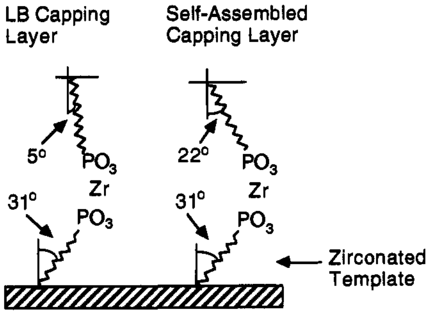

Scheme 3. Self-Assembly of Monolayer and Multilayered Films at the Zirconated LB Template

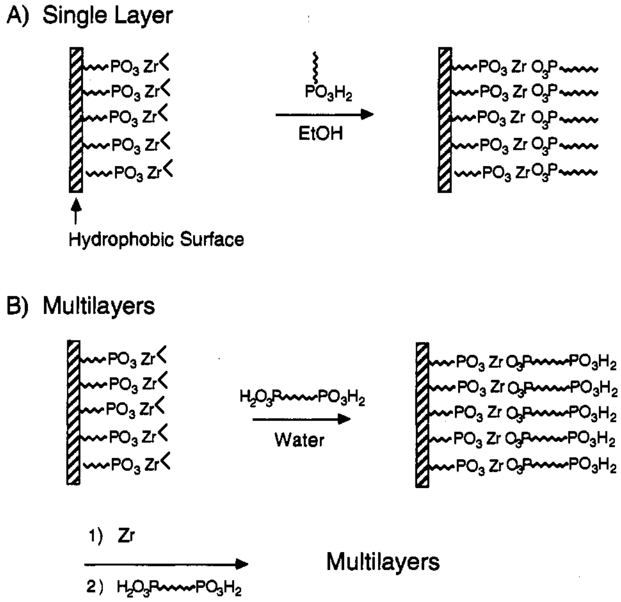

phosphonates allows this layer to be used in subsequent assembly steps without loss of organic film or displacement of zirconium ions.

Self-Assembly of Monolayers. Octadecylphosphonic acid is assembled to the zirconated LB template according to Scheme 3, completing the zirconium octadecylphosphonate bilayer. The zirconated surface is placed into a 1.25 mM (90:10 EtOH/H_2O) solution of the acid for 1 h and then removed, rinsed, and air-dried. Figure 1 compares the infrared spectra from 3100 to 2600 cm^{-1} of the zirconated LB template layer (top), the bilayer (middle), and the self-assembled octadecylphosphonic acid layer (bottom). The frequencies and fwhm's of each of the C–H stretching bands are the same in each spectrum, indicating that the conformational order and packing density of the alkyl chains in the film are preserved after the SA step. The IR intensities in the bilayer spectrum are double those of the template spectrum, indicating that the self-assembled layer contains the same amount of octadecylphosphonate as the zirconated LB template layer. This is further seen by comparing the top spectrum to the bottom spectrum in Figure 1, which is obtained by ratioing the self-assembled bilayer spectrum to the zirconated template layer spectrum. The frequencies, intensities, and peak shapes of the self-assembled layer are identical to those of the zirconated LB template layer, showing that the conformation and packing of the self-assembled layer are essentially equivalent to those of the LB layer.

The results of XPS analyses on the self-assembled octadecylphosphonic acid bilayer are listed in Table 2. For comparison, Table 2 also contains XPS data from an octadecylphosphonic acid bilayer formed by capping the zirconated LB template with another LB layer of octadecylphosphonic acid.[25] The observed Zr:P ratio corrected for the photoelectron attenuation lengths[13,35-38] for the self-assembled bilayer is 1:2 within experimental error.[37] The same ratio is found when the template is capped with an LB film[25] and is consistent with the stoichiometry of bulk zirconium phosphonates.[34,39] The Zr:P ratio supports the infrared data and shows that each Zr^{4+} site in the template binds an octadecylphosphonic acid molecule from solution.

Table 2. XPS Multiplex Data for Zirconium Phosphonate Layers

film type	elements	peak/area[a]	obsd rel intens[b]
zirconated LB template layer	Zr	Zr 3d/1306	53.0
	P	P 2p/215	47.0
self-assembled octadecylphosphonic acid bilayer	Zr	Zr 3d/3795	31.0
	P	P 2p/1589	69.0
Langmuir–Blodgett octadecylphosphonic acid bilayer	Zr	Zr 3d/919	33.1
	P	P 2p/345	66.9

[a] The units for area are (counts eV)/s. [b] Relative intensities are determined from experimental peak areas normalized with atomic and instrument sensitivity factors.[28,29]

Contact angle measurements on the self-assembled bilayer result in an advancing contact angle of 110 ± 1°, which is lower than the 112° contact angle observed when the zirconated LB template layer is capped with a second octadecylphosphonic acid LB monolayer.[25] Tilt angles of the alkyl chains, derived from polarized ATR-FTIR,[32,33] are listed in Table 1 and shown in Scheme 2. The tilt angles for the self-assembled and LB octadecylphosphonic acid capping layers are 22 and 5°, respectively. The 5° tilt angle of the LB capping layer is consistent with X-ray diffraction data from LB multilayers of zirconium octadecylphosphonate.[25] This nearly perpendicular arrangement of the alkyl chains accounts for the higher contact angle relative to that of the self-assembled layer. The surface pressure used to align the molecules in the LB experiment orients the alkyl chains nearly perpendicular to the surface,[25] and it appears that this packing is preserved when the layer is transferred to the zirconated LB template layer. Once the zirconium–phosphonate bond is formed, this extremely strong binding interaction does not allow the LB capping layer to relax. Since there is no pressure applied when the self-assembled layer is bound, this layer does not orient perpendicular to the surface. The higher tilt angle observed for the self-assembled capping layer is quite reasonable, given the size of the phosphonate head group, and is similar to the orientation of the alkyl chains seen in solid-state zirconium alkylphosphonates.[34,39] In fact, the bilayer formed by self-assembling the capping layer is closer to a single-layer analog of the solid-state zirconium phosphonates than the bilayer formed by LB methods alone.

Self-Assembly of Multilayered Films. Mallouk and coworkers[11-16] have demonstrated that the Zr–phosphonate interaction can be used to build multilayer films. We followed their procedure for depositing 1,10-decanediyldiphosphonic acid (DDPA) to build multilayer films at the zirconated LB template. A substrate coated with the zirconated LB template layer is placed in a 1.25 mM aqueous solution of DDPA for 1 h. The substrate is then rinsed with water, and multilayers are assembled by alternately repeating the Zr^{4+} ion and DDPA depositions.[11,12] The layer-by-layer deposition was monitored by ATR-FTIR, and Figure 2 shows the C–H stretching regions of the zirconated LB template layer (top), the template–DDPA bilayer (middle), and

---

(35) Seah, M. P.; Dench, W. A. *Surf. Interface Anal.* **1979**, *1*, 1–11.

(36) Brundle, C. R.; Hopster, H.; Swalen, J. D. *J. Chem. Phys.* **1979**, *70*, 5190–5196.

(37) *Practical Surface Analysis*; 2nd ed.; Briggs, D., Seah, M. P., Eds.; John Wiley and Sons: Chichester, U.K., 1990; Vol. 2, pp 240–245.

(38) Laibinis, P. E.; Bain, C. D.; Whitesides, G. M. *J. Phys. Chem.* **1991**, *95*, 7017–7021.

(39) Clearfield, A. *Comments Inorg. Chem.* **1990**, *10*, 89–128.

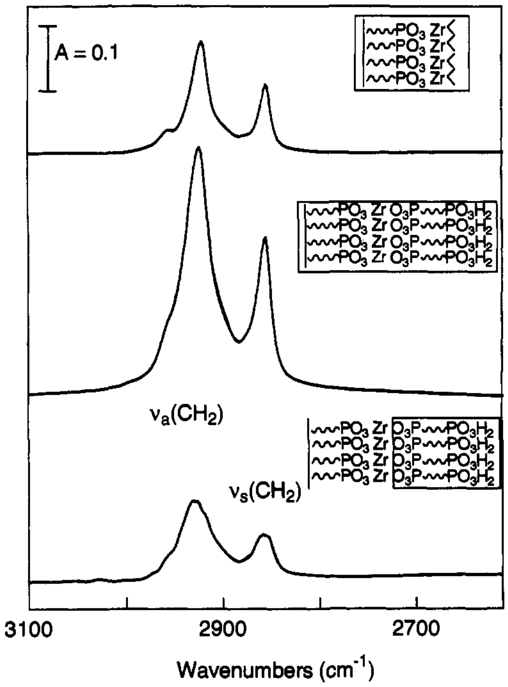

Figure 2. ATR-FTIR spectra monitoring the assembly of DDPA at the zirconated LB template: the zirconated template layer (top), the self-assembled DDPA–template bilayer (middle), the self-assembled DDPA layer (bottom). The $\nu_a(CH_2)$ band shifts to higher energy (2920 cm^{-1}) and broadens (30 cm^{-1}) upon formation of the self-assembled DDPA–template bilayer. The bottom spectrum is obtained by ratioing the top spectrum to the middle one to give the contribution due to the DDPA layer. The position and fwhm of the $\nu_a(CH_2)$ band are 2924 cm^{-1} and 41 cm^{-1}, respectively, indicating that a disorganized layer is formed.

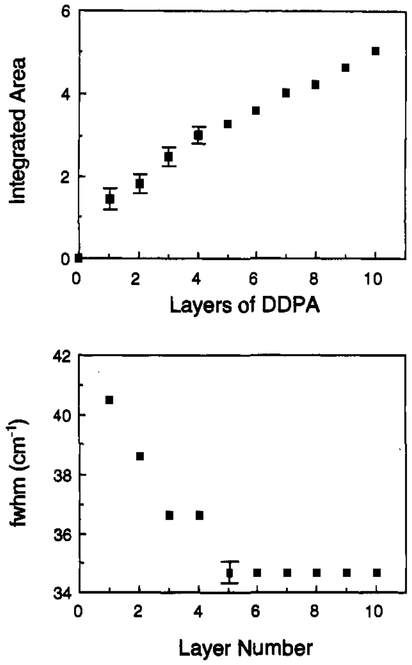

Figure 3. Plots of the intensity of the $\nu_a(CH_2)$ band versus the number of DDPA layers (top) and the fwhm of the $\nu_a(CH_2)$ for each DDPA layer (bottom) assembled at the zirconated LB template. The changes in the integrated area and the fwhm become constant after the fourth DDPA layer is assembled suggesting that at this point the same amount of material is now being deposited during each deposition cycle.

the self-assembled DDPA layer (bottom). The $\nu_a(CH_2)$ for the template–DDPA bilayer appears at a frequency of 2920 cm^{-1} and possesses a fwhm of 34.7 cm^{-1}. The increase in frequency and fwhm seen in the bilayer spectrum relative to that of the zirconated LB template layer indicates that more gauche bonds[5,30] are present in the bilayer and that the film is no longer close-packed.[5,31] The bottom spectrum in Figure 2 is for the DDPA layer only, which is obtained by ratioing the template–DDPA bilayer spectrum to the template layer spectrum. The DDPA IR spectrum indicates that this layer is disorganized. The frequency and fwhm of the $\nu_a(CH_2)$ are 2924 cm^{-1} and 41 cm^{-1}, respectively, which are similar to the values obtained from a solution spectrum of octadecylphosphonic acid[25] and correspond to a large percentage of gauche bonds[5,30] and loose packing of the alkyl chains.[5,31]

A plot of the integrated area of the $\nu_a(CH_2)$ band versus the number of layers of assembled DDPA (Figure 3 , top) shows a nonuniform increase in area with an increasing number of layers. The integrated area of $\nu_a(CH_2)$ for the first DDPA is much larger than that for the subsequent layers, although, after the fourth layer, the increase in area with each additional DDPA layer becomes constant. Figure 3 (bottom) is a plot of the fwhm for each individual DDPA layer assembled at the template. The fwhm decreases with the first four layers until it reaches a constant value of 34.7 cm^{-1}. The IR data suggest that once a DDPA molecule binds one end to the template layer, the exposed phosphonic acid group is able to bend over and bind another Zr^{4+} ion site within its reach, which is a consequence of the high density of Zr^{4+} ion binding sites in the zirconated template layer and the fact that DDPA is not a rigid molecule. The bridging of the Zr^{4+} ion sites by the DDPA molecules limits the number of sites available for binding in subsequent layers and accounts for the smaller increase in area of the $\nu_a(CH_2)$ band for each additional layer. After the fourth layer, however, a constant increase in area is observed, and the organization of each layer, as determined by the $\nu_a(CH_2)$ line shape, also becomes regular. At this point, it seems that the remaining available Zr^{4+} binding sites are spaced in such a manner that the bridging of these sites by the DDPA molecules is now less likely, and each subsequent assembly cycle deposits a constant amount of material, resulting in the layer-by-layer deposition observed by other workers using less ordered template layers.[11,12,16] However, the overall nonlinear increase in the area, coupled with the position and shape of the $\nu_a(CH_2)$ stretch, demonstrates that while a multilayered film is formed by self-assembling DDPA at the zirconated LB template, it is not a well-ordered, close-packed film.

Self-Assembly of Rigid Molecules. To avoid the possibility of bridging surface sites by the α,ω-diphosphonic acid molecules, we investigated layer-by-layer depositions of a rigid diphosphonic acid, quaterthiophenediphosphonic acid (QDP), developed by Katz.[21] Katz and co-workers[21] have shown that QDP can be self-assembled similarly to the α,ω-alkyldiphosphonic acid molecules. QDP is self-assembled at the zirconated LB template from a 1 mM 50:50 DMSO/H_2O solution of QDP that is adjusted to pH 3 with a 10% solution of HCl. Depositions are carried out at 25 °C for 1 h, and then the films are rinsed with a 50:50 DMSO/H_2O solution, followed by a second rinse with pure water to remove any excess material. Previous work[21] involving the self-assembly of QDP indicated that elevated temperatures were needed to overcome steric barriers, although the data below demonstrate that QDP molecules can be self-assembled at room temperature. The difference may be that the close-packing of the LB layer prohibits any of the surface groups from being buried in the organic layer, thereby allowing the QDP molecules to access more Zr^{4+} sites at the surface.

The layer-by-layer assembly of QDP was monitored by UV–vis spectroscopy with the incident beam perpendicular to the substrate. There is no change in the UV–vis spectrum when the time of deposition is increased, suggesting that the deposition is complete after 1 h. This is confirmed by XPS, which shows that, for deposition times of 1 and 7 h, the Zr:P:S ratios[40] are the same within experimental error.[37] A plot of the UV–vis absorbance at 390 nm versus the number of self-assembled QDP layers is

---

(40) Byrd, H.; Whipps, S.; Pike, J. K.; Talham, D. R. Unpublished results.

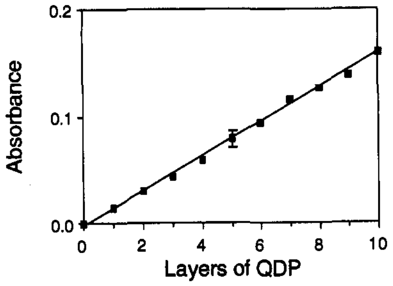

Figure 4. Absorbance at 390 nm versus the number of layers of QDP assembled at the zirconated LB template. The linear increase indicates the same amount of material is deposited during each deposition cycle. The solid line is a linear regression fit to the data.

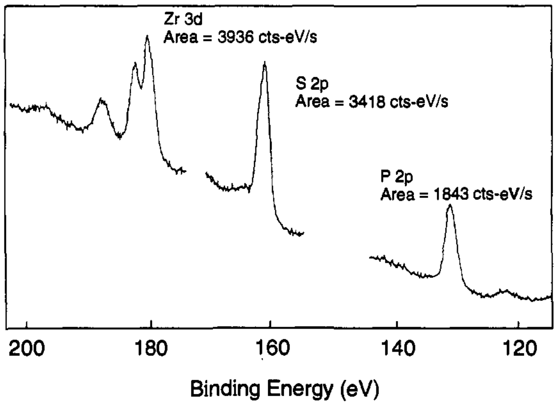

Figure 5. XPS multiplex spectrum for one layer of QDP assembled at the zirconated LB template. The ratio of the observed relative intensities for Zr:P:S is 1:2.5:3.2. A matrix model developed from the attenuation equation, described in the text, was used to predict the percent coverage of QDP molecules. From this model, the coverage of QDP molecules corresponds to approximately 60–80% of the Zr^{4+} sites in the template layer binding QDP molecules from solution.

shown in Figure 4. The linear increase in absorbance demonstrates that the same amount of QDP is deposited during each cycle. The UV–vis absorbance per QDP layer is less than what has been previously reported.[21] The transition moment for the 390-nm band is parallel with the molecular axis,[41,42] and the lower absorbance in the transmission experiment is consistent with the average orientation of the QDP molecular axis approaching the surface normal.

Figure 5 shows an XPS multiplex spectrum for a single layer of QDP self-assembled onto the zirconated LB template. From an XPS survey scan, C, O, P, S, Zr, and Si (from the substrate) are the only elements present at the surface.[40] The multiplex spectrum reveals a Zr:P:S ratio of 1:2.5:3.2. A model was derived from the attenuation equation[37] in order to predict the relative elemental intensities of Zr, P, and S in the sample. The distance of each element from the outermost surface is calculated from known interatomic distances,[21,43] assuming vertical orientation of the QDP molecules with respect to the substrate plane. The result is a model matrix in which there are discrete layers of elements each separated by some distance, d, from the outermost surface. Each atom, A, in the sample will contribute a term

$$I_A = I_A^{\infty} \exp(-d_m/(\lambda_m \sin \Theta))$$

to the spectrum[37] in which I_A^{∞} is the peak area normalization or sensitivity factor,[28] d_m is the overlayer thickness of material m, in this case the QDP layer, λ_m is the inelastic mean free path of the photoelectron through material m, and Θ is the takeoff angle with respect to the surface parallel. The above term gives a calculated relative intensity, I_A, of element A when multiplied by a stoichiometric factor and summed over each A-containing layer in the matrix. The inelastic mean free path, λ_m, is dependent upon the kinetic energy of the photoelectron and upon the material through which the escaping photoelectron travels. For organic layers, literature values of λ_m vary by about an order of magnitude.[13,35,36,38,44–46] For 100% coverage (i.e., one template Zr^{4+} ion binds one QDP molecule), one expects a Zr:P:S ratio of between 1.0:3.8:5.5 and 1.0:3.1:4.2 for low[35] and high[13] values of λ_m, respectively. These ratios are not observed, and we conclude that our reported Zr:P:S ratio of 1:2.5:3.2 is consistent with a QDP coverage of approximately 60–80%, depending upon the value of λ_m chosen. In addition, as an internal check, the relative ratio of P to S is consistent with QDP adsorbing to the surface without trapping excess DMSO in the film. The incomplete coverage of the QDP molecules is perhaps explained by the mismatch between the cross-sectional molecular areas of the Zr^{4+} ion sites and the QDP molecules. The area per binding site for the zirconated LB template is dictated by the cross-sectional area per molecule of the LB octadecylphosphonic acid film,[25,47] which is 24 Å^2, whereas the calculated cross-sectional area for the QDP molecule[48] is approximately 28 Å^2.

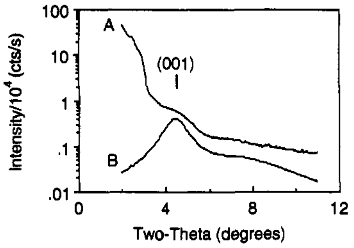

Figure 6. Low-angle X-ray diffraction from 10 layers of QDP assembled at the zirconated LB template. Curve A is a plot of the experimental data. Curve B is a plot of two Lorentzian curves derived from a fit of the experimental data (see text). The peak at 2θ = 4.37° is assigned to the (001) reflection and corresponds to a d spacing of 20.19 Å.

X-ray diffraction from 10 layers of QDP assembled at the zirconated LB template is shown in Figure 6. The experimental data are fit by superimposing two Lorentzian peaks onto a background that was modeled by the sum of a zero-point Lorentzian plus a quadratic contribution due to diffuse scattering. The peak at a 2θ value of 4.37° can be assigned to the (001) reflection and corresponds to a d spacing of 20.19 Å. A second order reflection is also seen. The d spacing for the QDP multilayer film agrees well with the size of the QDP molecule.[21] If the QDP molecules are oriented exactly perpendicular to the surface, a d spacing of 21 Å is predicted.[21] The observed d spacing suggests that the QDP molecules are slightly tilted from the surface normal.

The interlayer coherence length (L) can be estimated using the Scherrer formula[49]

$$L = 0.94\lambda/(B(2\theta)\cos\theta_B)$$

where λ is the wavelength of the X-ray, $B(2\theta)$ measured in radians is the fwhm of the 2θ peak, and θ_B is the Bragg angle for the peak. Using a fwhm of 0.0109 radian, taken from the fitted data for

---

(41) Schoeler, U.; Tews, K. H.; Kuhn, H. *J. Chem. Phys.* **1974**, *61*, 5009–5015.

(42) Eckert, R.; Kuhn, H. *Z. Elektrochem.* **1960**, *64*, 356–364.

(43) Poojary, M. D.; Hu, H.; Campbell, I.; F. L.; Clearfield, A. *Acta Crystallogr.*, in press.

(44) Sastry, M.; Ganguly, P.; Badrinarayanan, S.; Mandale, A. B.; Sainkar, S. R.; Paranjape, D. V.; Patil, K. R.; Chaudhary, S. K. *J. Chem. Phys.* **1991**, *95*, 8631–8635.

(45) Nesternenko, B.; Milenen, V.; Gorkun, O.; Stadnik, A.; Kazantsera, Z.; Nabok, A. *Thin Solid Films* **1991**, *201*, 351.

(46) Ohnishi, T.; Ishitani, A.; Ishida, H.; Yamamoto, N.; Tsubomura, H. *J. Phys. Chem.* **1978**, *82*, 1989–1991.

(47) Byrd, H.; Pike, J. K.; Talham, D. R. *Thin Solid Films*, *in press*.

(48) Tasaka, S.; Katz, H. E.; Hutton, R. S.; Orenstein, J.; Fredrickson, G. H.; Wang, T. T. *Synth. Met.* **1986**, *16*, 17–30.

(49) Cullity, B. D. *Elements of X-Ray Diffraction*; Addison-Wesley Publishing Co.: Reading, MA, 1956.

the (001) reflection, a coherence length of 133 Å is obtained, which corresponds to six or seven layers. This is consistent with the broad (002) reflection and the Lorentzian line shapes and is reasonable for a 10-layer film if we consider that the first and last layers probably assume a different packing than the bulk. X-ray diffraction demonstrates that layered films can be produced using one-layer-at-a-time self-assembly deposition methods.[14] The close-packed LB template layer appears to orient the QDP molecules nearly perpendicular to the surface such that well-ordered layers can be assembled, even though the mismatch in area between the Zr^{4+} sites in the zirconated LB template and the QDP molecules hinders the formation of a more organized film. It seems reasonable that the use of a template molecule that results in a Zr^{4+} ion spacing closer to the QDP cross-sectional area could result in a more crystalline film.

Conclusions

In conclusion, a zirconated octadecylphosphonic acid LB film provides an organized and well-defined surface for assembling organophosphonate molecules from solution. When octadecylphosphonic acid is assembled at the zirconated LB template, a zirconium phosphonate bilayer is formed with the self-assembled layer assuming an organization similar to that of the original LB template layer. The order of the template is transferred to the self-assembled layer. The bilayer formed by self-assembling octadecylphosphonic acid on the zirconated LB template provides a good single-layer analog of layered solid-state zirconium phosphonates. Multilayers can also be produced at the LB template by self-assembling α,ω-diphosphonic acid molecules. If the diacid molecule is rigid, a well-defined layered structure can be produced. In the multilayers formed from QDP, the interlayer spacing, determined by X-ray diffraction, is comparable to the length of the QDP molecule. Because the zirconated LB surface is close-packed and inflexible, the QDP packing density is limited by the cross-sectional area of the QDP molecule. The incommensurate sizes of the LB template molecules and the QDP molecule, however, probably limit the in-plane order that can be achieved with this system. In the case of 1,10-decanediyldiphosphonic acid, where the diacid molecule is flexible, multilayer films can also be produced although the layered nature of these films is less well defined. Initially, the flexible α,ω-diphosphonic acid molecules bridge Zr^{4+} sites in the template layer, therefore reducing the density of binding sites available in subsequent layers. Finally, a well-characterized and -organized LB template layer can play an important role in understanding and quantifying layer-by-layer self-assembly. For applications where controlling the architecture, order, and density of molecules within layered assemblies is required, the organization of the template layer is important.

Acknowledgment. We thank Dr. Howard Katz for providing the sample of quaterthiophenediphosphonic acid and for providing a copy of ref 18 prior to publication. We also thank Professor Vince Cammarata for assistance with the polarized ATR-FTIR experiment, Professor Kirk S. Schanze for use of the UV–vis spectrometer, and the Major Analytical Instrumentation Center at the University of Florida for instrument time. Acknowledgment is made to the National Science Foundation [DMR-9205333], and the University of Florida Division of Sponsored Research for partial support.